Measurement of the flow velocity field in multi–field wire–plate electrostatic precipitator

J. Podlinski, J. Dekowski, M. Kocik, J. Mizeraczyk

Centre for Plasma and Laser Engineering,
The Szewalski Institute of Fluid–Flow Machinery, Polish Academy of Sciences,
Fiszera 14, 80–231 Gdańsk, Poland

J. S. Chang

Department of Engineering Physics, McMaster University,
Hamilton, Ontario, Canada L8S 4L7

Received 29 April 2004

In this paper results of Particle Image Velocimetry (PIV) measurements of the particle flow velocity fields in a wire–to–plate type electrostatic precipitator (ESP) are presented. One or two grounded stainless–steel plate electrodes and seven wire electrodes in the middle of the ESP height were used. The measurements were carried out in the plane placed perpendicularly to the wire electrodes (for the ESP version with two plate electrodes) and in four planes placed parallel to the wire electrodes (for the ESP version with one plate electrode). Either negative or positive voltage polarity was applied to the wire electrodes. The main gas flow velocity was 0.14 m/s.

The obtained results showed strong influence of the electrohydrodynamic (EHD) forces on the flow patterns, which exhibited strong upstream and downstream vortexes. The experiment confirmed that the flow patterns in the ESP have 3–dimensional character.

PACS: 47.65.+a, 52.30.Cv, 52.25.Fi
Key words: electrostatic precipitator, corona discharge, EHD flow, flow measurement, PIV

1 Introduction

Electrostatic precipitators (ESPs) operate with overall collection efficiency higher than 99%. The non–collected part consists mainly of fine particles (micron and submicron sizes), which may contain toxic trace elements [1]. Therefore, removal of fine particles from flue gases in ESPs is still an important issue. The precipitation of the particles in ESPs depend on the particle properties, electric field, space charge, ESP design and gas flow field [2]. To elucidate the influence of the electrically generated flow disturbances on the gas cleaning process, the flow patterns in the ESPs were studied using various visualization and laser techniques [3–7].

In this paper results of the Particle Image Velocimetry (PIV) measurements of the particle flow velocity fields in a wire–to–plate type ESP are presented.

2 Experiment

In general, the flow pattern in the ESP has 3–dimensional character [3, 8]. At present, imaging of the 3–dimensional velocity field in the ESP is very difficult. However, measurements of the velocity fields in several planes in perpendicular and parallel cross sections

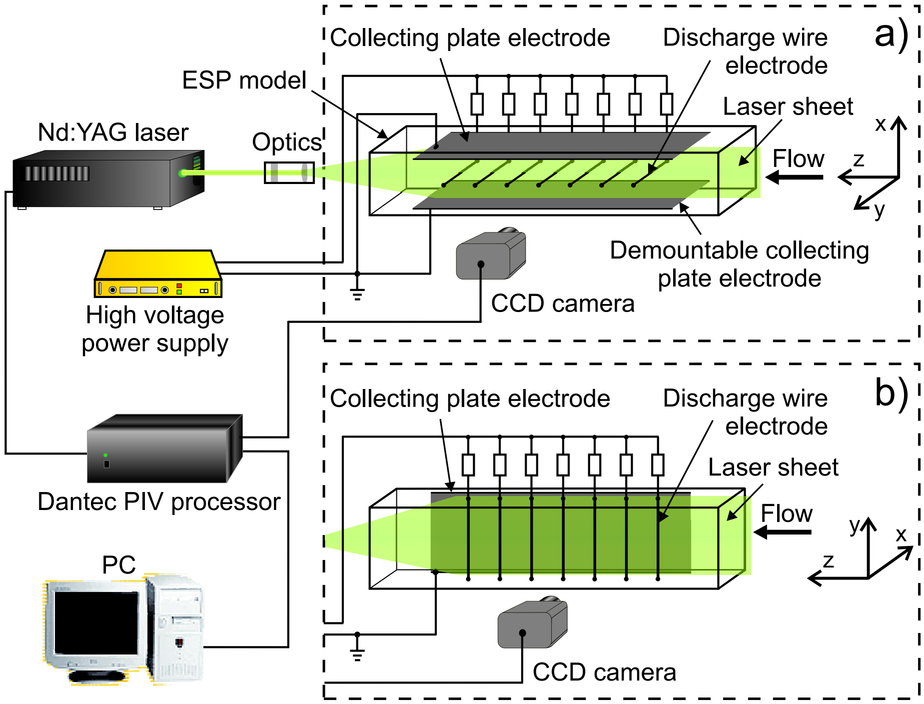

Fig. 1. Experimental setup for measurements of the velocity field in the ESP:
a) perpendicular section (two plate electrodes present)
b) parallel section (single plate electrode present).

in the ESP are feasible. Such measurements could be quite informative on the spatial characteristics of the flow in the ESP, although being far from the full picture which can be obtained from 3–dimensional measurements.

In this experiment we aimed at measuring the velocity field in one plane perpendicular to the wire and plate electrodes (a perpendicular section, the first experiment) and in several planes parallel to both electrodes (parallel sections, the second experiment). However, the latter measurement was not feasible when both plate electrodes were present in the ESP because the opaque plate electrode protrudes observation of the flow pattern in the planes parallel to the electrodes. Therefore, we could measure the velocity field in the planes parallel to the electrodes only when one of the plate electrode was removed. Accordingly, in the second experiment we used an ESP version with one plate electrode only.

The apparatus used in this experiment consisted of an ESP, high voltage supply and standard PIV equipment for the measurement of velocity field (Fig. 1).

In the first experiment, when the velocity field was measured in the perpendicular section, the ESP was a plane–parallel acrylic duct, 200 mm wide, 160 mm high, and 1600 mm long (Fig. 1a). In the centre of the duct, at the top and bottom acrylic walls two collecting stainless–steel plate electrodes (200 mm × 1000 mm) were mounted. The distance between plate electrodes was 100 mm. In the middle between the plate electrodes seven stainless–steel wire electrodes (diameter of 1 mm, length of 200 mm) were placed, parallel to the plate electrodes (Fig. 1a). They were fixed in the acrylic side–walls. The distance between wire electrodes was 100 mm and the distance from each wire to the plate electrodes was 50 mm.

In the second experiment, when the velocity field was measured in the parallel sections, the same plane–parallel acrylic duct was used. However, one of the plate electrodes was removed to make the observation of the flow in the parallel sections possible (Fig. 1b). After removing one of the plate electrodes, the distance between the wire electrodes and the acrylic wall was 80 mm.

The absence of the second plate electrode influenced apparently the velocity field patterns in the ESP, which are supposed to be different to those in a typical ESP with two–plate electrodes, in particular in the space between the wires and the acrylic wall. On the other hand, however, we expected that main features of the velocity field patterns of the typical ESP with two plate electrodes should be preserved to same extend in the space between the wires and the plate electrode in our single–plate ESP.

The voltage applied to the wire electrodes was 24 kV for the ESP with two plate electrodes. The discharge current was 580 μA for negative polarity and 650 μA for positive polarity. For the ESP with single plate electrode a voltage of 26 kV was applied. The discharge current was 520 μA for the negative polarity and 540 μA for the positive polarity. The mentioned voltage, measured just after the power supply, was supplied to each wire through a 10 MΩ resistor. Air seeded with cigarette smoke (size of less than 1 μm in dry air) was blown through the ESP duct with an average velocity of 0.14 m/s.

The PIV equipment consisted of a twin second harmonic Nd–YAG laser system (λ = 532 nm, pulse energy 50 mJ), imaging optics (cylindrical telescope), CCD camera, image processor (Dantec PIV 1100) and PC computer. The laser sheet of thickness of 1 mm, formed from the Nd–YAG laser beam by the cylindrical telescope was introduced into the ESP to form observation planes. The particle images were recorded by the Kodak Mega Plus ES 1.0 CCD camera. The captured images were transmitted by the Dantec PIV 1100 image processor to the PC computer for digital analysis.

The laser sheet of a thickness of 1 mm was placed either perpendicularly to the wire electrodes at their half–length (measurement in the perpendicular section when the ESP had two plate electrodes, Fig. 1a) or parallel to the wire electrodes (measurement in the parallel sections when the ESP had only single plate electrode, Fig. 1b). The parallel planes of observation were set at four distances from the wires, forming a plane I – between the acrylic wall and the wires at $x = -25$ mm, and planes II, III and IV – between the wires and the plate electrode at $x = 5$ mm, $x = 25$ mm and $x = 45$ mm, respectively (x– distance from the wire electrodes, Fig. 3).

The velocity field maps presented in this paper are composed of several adjacent velocity fields (in Fig. 3 they are marked as rectangular A–G. All the velocity fields resulted from the averaging of 100 measurements, which means that each presented velocity field is time–averaged.

3 Results

When the PIV method is used for monitoring the flow in which electric forces exist, the obtained velocity field shows the flow structure changed by the electrohydrodynamic (EHD) forces [5–7].

3.1 Flow patterns in the section perpendicular to the wires

The flow velocity field measured by the PIV and the corresponding streamlines in the section perpendicular to the wires in the ESP with seven negatively polarized wire electrodes and two plate electrodes are shown in Fig. 2.

We observed that at a relatively low primary flow velocity (0.14 m/s) the seed particles were removed very fast from the gas even at a relatively low voltage (24 kV). The particle removal was higher with increasing distance from the first wire electrode downstream. Beyond the third wire electrode the gas was almost free from the seed particles, which caused the PIV measurement impossible to be carried out beyond the third wire downstream. Therefore, the flow velocity field and streamlines in Fig. 2 are limited only to the area with 3 first electrodes.

At a primary flow average velocity of 0.14 m/s, the Reynolds number was $Re = 466$; the EHD number $E_{\mathrm{hd}} = 3.3 \times 10^6$, and the ratio of the EHD number to the Reynolds number squared $E_{\mathrm{hd}}/Re^2 = 15.2$ [9]. The parameters used to calculate Re and E_{hd} were: primary flow velocity $V = 0.14$ m/s, air dynamic viscosity $\nu = 15 \times 10^{-6}$ m^2/s, air density $\rho = 1.205$ kg/m^3, ion mobility (N_2^+ in air) $\mu_{\mathrm{i}} = 2.93 \times 10^{-4}$ m^2/Vs, characteristic length (wire–plate distance) $L = 0.05$ m, discharge area (covered by 7 wire electrodes on two plate electrodes) $A = 2 \times 700\,\mathrm{mm} \times 200\,\mathrm{mm} = 0.28\,\mathrm{m}^2$, total discharge current $I = 580\,\mu\mathrm{A}$. Since the $E_{\mathrm{hd}}/Re^2 \gg 1$, the electric force was dominating over the inertial one, disturbing heavily the primary flow. Strong vortexes (with local velocities up to 0.45 m/s) were formed in both the upstream and the downstream regions of the ESP (Figs. 2a and b). The upstream region vortexes, with their centres placed around 60 mm from the first wire electrode, were stable and regular.

The flow patterns measured in the ESP with two plate electrodes and seven positively polarized wire electrodes are very similar to those under negative polarity. For the total discharge current $I = 650\,\mu\mathrm{A}$ and the other parameters as for the negative polarity the Reynolds number was $Re = 466$, the EHD number $E_{\mathrm{hd}} = 3.7 \times 10^6$, and the ratio of the EHD number to the Reynolds number squared $E_{\mathrm{hd}}/Re^2 = 17$. Therefore, also under positive polarity the electric force dominated over the inertial one, forming, as experimentally observed by us, strong vortexes in both the upstream and the downstream regions of the ESP.

3.2 Flow patterns in the sections parallel to the wires

The streamlines in the four parallel planes in the ESP with seven positively polarized wire electrodes and single plate electrode are shown in Fig. 3. The streamlines were drawn basing on the corresponding measured PIV velocity fields.

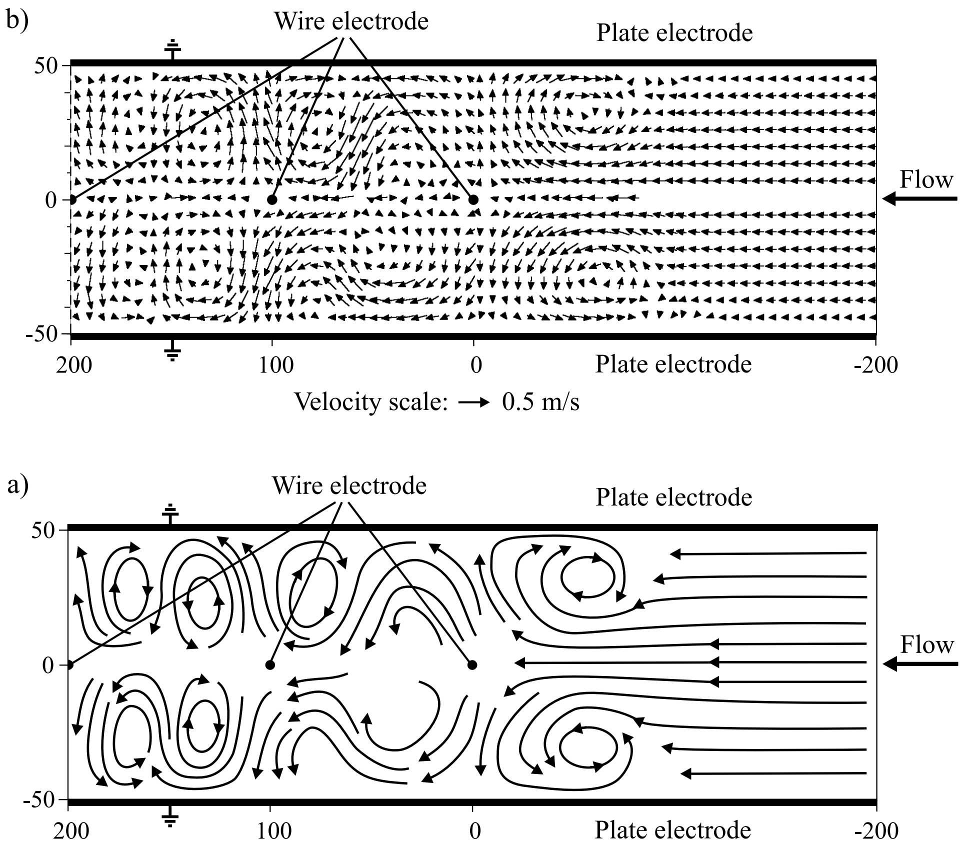

Fig. 2. Flow velocity field (a) and schematic streamlines (b) in the ESP with 7 wire electrodes and 2 plate electrodes (only the area with 3 first electrodes). Primary flow average velocity of 0.14 m/s, applied negative voltage of 24 kV, discharge current of 580 μA. The observation plane was placed perpendicularly to the wire electrodes at their half–length. Positions of the wires are marked by dots. Dimensions in mm.

In the ESP with single plate electrode the particle removal was not so efficient as in the ESP with two plate electrodes, so the seed particles were present in whole ESP reactor. Therefore, we were able to measure the flow velocity field in the area ranged up to the last, seventh wire electrode

At a primary flow average velocity of 0.14 m/s, discharge area (covered by 7 wire electrodes on the single plate electrode) $A = 700\,\mathrm{mm} \times 200\,\mathrm{mm} = 0.14\,\mathrm{m}^2$, total discharge current $I = 540\,\mu\mathrm{A}$, and the other parameters as for the ESP with two plate electrodes, the Reynolds number was $Re = 466$, the EHD number $E_{\mathrm{hd}} = 6.1 \times 10^6$, and the ratio of the EHD number to the Reynolds number squared $E_{\mathrm{hd}}/Re^2 = 28$. As in the ESP with two plate electrodes, the $E_{\mathrm{hd}}/Re^2 \gg 1$. Therefore, the flow between the wires and the plate is supposed to be influenced by the EHD forces.

The influence of the EHD forces on the flow structure is clearly seen in Fig. 3. The weakest influence of the EHD forces on the flow is seen in the plane I ($x = -25$ mm), situated in the space between the wire electrodes and the acrylic sidewall, i.e. outside of the discharge area. In the area D of the plane I the EHD forces caused the gas to move opposite to the direction of the primary flow. This opposite flow seems to be a cause of small vortexes seen in the areas B and C.

In the plane II ($x = 5$ mm) the influence of the EHD forces is greater than in the plane I. A pair of large vortexes near the wire electrode No. 1 (the area B) and large areas without vortexes in the plane II near the wire electrodes No. 3–7 are seen. In the area A (upstream from the wire electrode No. 1), the gas is forced to flow against the primary gas flow direction.

In the plane III ($x = 25$ mm) a pair of vortexes in the transit area between A and B (similarly as in the plane II) and pairs of vortexes in the areas E, F, G (corresponding to the wire electrodes No. 4–7) are present. In the area A, the gas flows opposite to the direction of the primary gas flow.

In the plane IV ($x = 45$ mm, situated 5 mm before the plate electrode) strong flow along the plate electrode, directed either in accord with or against the direction of the primary flow, are present. This is understandable, assuming that there is a strong flow from each wire electrode perpendicularly to the plate electrode. Such a flow has to break up before the plate electrode into streams flowing along the plate electrode. This actually happens already in the plane IV, where the flow from each wire electrode diverts downstream and upstream, resulting in several flow moving upstream and downstream. In the area A a strong flow moves oppositely to the direction of the primary gas flow, resulting in vortexes around $z = -200$ mm.

In each measured plane, the flow patterns in areas E, F and G (corresponding to the wire electrodes No. 5–7 are similar. It seems that in these areas the regular and reproducible flow patterns are formed, while the transit areas A–D, corresponding to the wire electrodes No. 1–4 exhibit irregular flow patterns. We may anticipate that the regular flow patterns seen in the areas E–G would be reproduced if the wire electrode number is larger than 7.

The flow patterns in the same four parallel planes were also measured in the ESP with seven negatively polarized wire electrodes and one plate electrode. For the total discharge current $I = 520\,\mu$A and the other parameters as for the positive polarity; the Reynolds number was $Re = 466$, the EHD number $E_{\mathrm{hd}} = 5.9\times10^6$, and the ratio of the EHD number to the Reynolds number squared $E_{\mathrm{hd}}/Re^2 = 27$. Therefore, under the negative polarity the EHD forces were expected to be strong in the ESP.

Also under the negative polarity the vortexes are formed in the ESP, the gas is forced to flow against the primary gas flow direction in the area A (planes I, II and III), and in the plane IV strong flow along the plate electrode are present. However, all the flow patterns are less symmetrical and regular than for the positive polarity. Under the negative polarity the flow patterns in areas E, F and G in each measured plane are not as similar to each other as for the positive polarity.

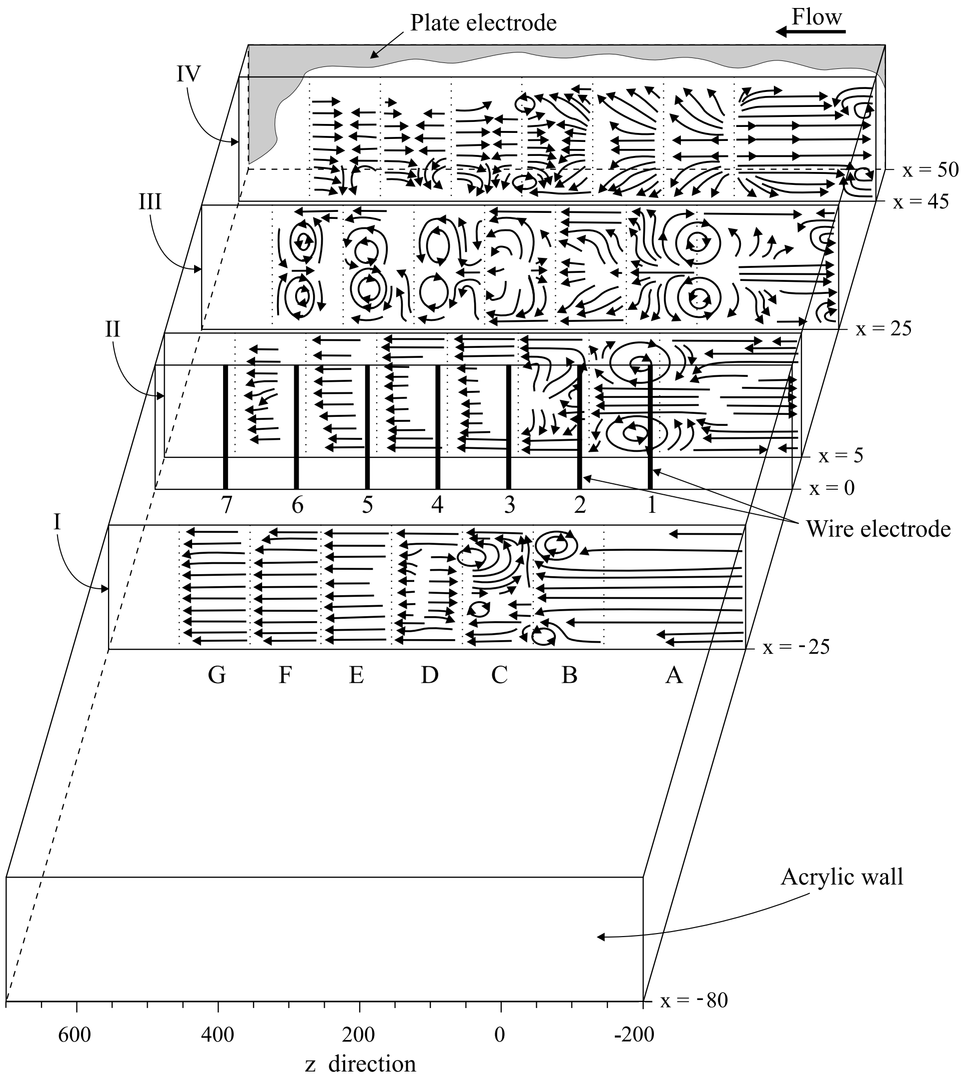

Fig. 3. Schematic streamlines in the ESP with seven wire electrodes and one plate electrode at a primary flow average velocity of 0.14 m/s, applied positive voltage of 26 kV, discharge current of 540 μA. The observation planes were placed parallel to the wire electrodes. Dimensions in mm, *x* – distance from the wire plane. A–G – measurement subareas, 1–7 – wire electrode numbering.

3.3 Outline of the flow velocity field in an ESP

The following three–dimensional outline of the vortexes in the ESP with seven positively polarized wire electrodes and single plate electrode as in Fig. 4 (only region around wires No. 4–7 is shown) can be deduced from the measurements presented above. The vortexes

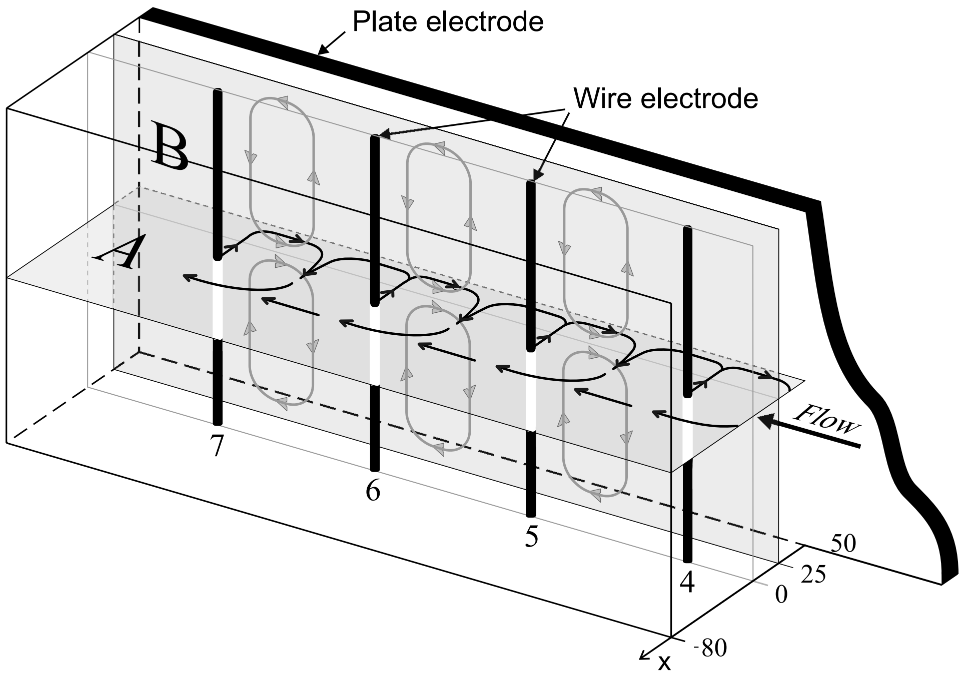

Fig. 4. 3D outline of the vortexes in planes A and B (shaded) around the wires No. 4–7 in the ESP with positive polarity.

drawn in plane A (situated perpendicularly to the wire electrodes at their half–length) are deduced from the experimentally measured velocity fields in this plane and the results presented in Fig. 3. The vortexes drawn in the plane B (situated parallel to the wire electrodes, 25 mm before the plate electrode) correspond to the results presented in Fig. 3 (plane III).

The 3D flow pattern outline based on the experimental results presented in this paper shows that the flow in the ESP is complex, with vortexes in the planes parallel and perpendicular to the wire electrodes. This is in agreement with the results presented in [3].

4 Summary and conclusions

In this paper the flow velocity fields and streamlines measured by the PIV in the wire–to–plate type ESP are presented. The ESP had seven wire electrodes and one or two plate electrodes. Either negative or positive voltage polarity was applied to the wire electrodes. The measurement planes were placed either perpendicularly to the wire electrodes at their half–length or in four planes parallel to the wire electrodes.

The presented results confirmed that the presence of the electric field causes significant changes in the flow patterns in the ESP. In the ESP with a primary flow average velocity of 0.14 m/s, the EHD induced secondary flow (having velocity of several tens of cm/s) with strong vortexes in the downstream and upstream regions is formed.

This investigations confirmed that the flow patterns in the ESP are 3–dimensional as shown in previous publications [3, 8].

The present experiment showed a complex nature of the EHD–induced secondary flow in the ESPs, and pointed out the necessity of 3–dimensional measurements of the velocity fields to reveal this complexity.

This work was supported by the Foundation for Polish Science (FNP, subsidy 8/2001) and the Institute of Fluid Flow Machinery (grant IMP PAN O3/Z–3/T2).

References

[1] A. Mizuno: IEEE Trans. on Dielectrics and Electrical Insulation **5–7** (2000) 615–624.

[2] P. Atten, F. M. J. McCluskey, A. C. Lahjomri: IEEE Trans. Ind. Appl. **23–4** (1987) 705–711.

[3] G. A. Kallio, D. E. Stock: IEEE Trans. Ind. Appl. **26–3** (1990) 503–514.

[4] S. J. Park, S. S. Kim: Aerosol Science and Technology **33 (3)** (2000) 205–221.

[5] J. Mizeraczyk, M. Kocik, J. Dekowski, M. Dors, J. Podlinski, T. Ohkubo, S. Kanazawa, T. Kawasaki: J. Electrostatics **51–52** (2001) 272.

[6] J. Mizeraczyk, J. Dekowski, J. Podlinski, M. Kocik, T. Ohkubo, S. Kanazawa: J. Visualization **6, 2** (2003) 125–133.

[7] M. Kocik, J. Podlinski, J. Dekowski, M. Dors, J. Mizeraczyk: Proc. SPIE **5229** (2003) 301–304.

[8] T. Yamamoto, M. Okuda, M. Okubo: IEEE Trans. Ind. Appl. **39, 6** (2003) 1602–1607.

[9] IEEE–DEIS–EHD Technical Committee: IEEE Trans. Dielectrics and Electrical Insulation **10–1** (2003) 3–6.